Biomaterials 46 (2015) 58–69

Contents lists available at ScienceDirect

Biomaterials

journal homepage: www.elsevier.com/locate/biomaterials

Biotechnological approach for systemic delivery of membrane Receptor Activator of NF-κB Ligand (RANKL) active domain into the circulation

Alfredo Cappariello [a], Riccardo Paone [b], Antonio Maurizi [b], Mattia Capulli [b], Nadia Rucci [b], Maurizio Muraca [a], Anna Teti [b, *]

[a] Regenerative Medicine Unit, Ospedale Pediatrico Bambino Gesù Istituto di Ricovero e Cura a Carattere Scientifico, Piazza S. Onofrio 4, 00165 Rome, Italy
[b] Department of Biotechnological and Applied Clinical Sciences, University of L'Aquila, Via Vetoio – Coppito 2, 67100 L'Aquila, Italy

ARTICLE INFO

Article history:
Received 23 September 2014
Accepted 20 December 2014
Available online

Keywords:
Receptor Activator of NF-κB Ligand
RANKL
Osteoclast
Osteopetrosis
Diffusion chambers

ABSTRACT

Deficiency of Receptor Activator of NF-κB Ligand (RANKL) prevents osteoclast formation causing osteopetrosis. RANKL is a membrane-bound protein cleaved into active soluble (s)RANKL by metalloproteinase 14 (MMP14). We created a bio-device that harbors primary osteoblasts, cultured on 3D hydroxyapatite scaffolds carrying immobilized MMP14 catalytic domain. Scaffolds were sealed in diffusion chambers and implanted in RANKL-deficient mice. Mice received 1 or 2 diffusion chambers, once or twice and were sacrificed after 1 or 2 months from implants. A progressive increase of body weight was observed in the implanted groups. Histological sections of tibias of non-implanted mice were negative for the osteoclast marker Tartrate-Resistant Acid Phosphatase (TRAcP), consistent with the lack of osteoclasts. In contrast, tibias excised from implanted mice showed TRAcP-positive cells in the bone marrow and on the bone surface, these latter morphologically similar to mature osteoclasts. In mice implanted with 4 diffusion chambers total, we noted the highest number and size of TRAcP-positive cells, with quantifiable eroded bone surface and significant reduction of trabecular bone volume. These data demonstrate that our bio-device delivers effective sRANKL, inducing osteoclastogenesis in RANKL-deficient mice, supporting the feasibility of an innovative experimental strategy to treat systemic cytokine deficiencies.

1. Introduction

Systemic delivery of cytokines could be an innovative treatment for genetic diseases characterized by failure in cytokine pathways [1]. However, this treatment could be cumbersome for many reasons. They include i) the lack of industrial interest to develop pharmaceutical formulations of a cytokine that should be available only for a limited number of patients, ii) the demanding compliance because of the parenteral route of administration, and iii) the difficulty to adjust the dose according to the real status of the disease.

Long-lasting delivery of a cytokine through a regulated biological system would be ideal to prevail over these inconveniences. Several cytokines are released by cells originating from the mesenchymal stem cell family [2] under the control of local and systemic regulating pathways, which makes this cell family a superlative tool if transplanted in vivo. However, although intense research is ongoing for the development of transplant procedures for mesenchymal stem cells, so far, the experimental efforts did not lead to satisfactory engraftment [3,4], therefore this option remains currently unfeasible.

Some cytokines are membrane-bound proteins that require cell–cell contact or ectodomain shedding to exert their action. For instance, the Receptor Activator of Nuclear Factor-κB transcription factor Ligand (RANKL) is a trimeric cytokine belonging to the Tumor Necrosis Factor (TNF) family [5], which exhibits potent osteoclastogenic properties [6]. In bone, it is expressed by the osteogenic lineage [7] as a surface protein and is known to trigger osteoclast formation upon exposure of bone marrow mononuclear cells to the Macrophage-Colony Stimulating Factor (M-CSF) [8], another essential cytokine that promotes proliferation of osteoclast precursors [9], and sensitizes them to RANKL inducing the expression

* Corresponding author. Tel.: +39 0862 433511, +39 0862 433513; fax: +39 0862 433523.
E-mail address: annamaria.teti@univaq.it (A. Teti).

http://dx.doi.org/10.1016/j.biomaterials.2014.12.033

of the RANKL receptor, RANK [10]. RANKL has also emerged to play many roles in other organs [11]. It is produced by T-cells in response to inflammatory stimuli, enhancing osteoclast activity in inflammatory diseases such as the rheumatoid arthritis [12,13]. It also regulates mammary gland development [14] and is involved in mammary gland tumorigenesis [15]. Finally, RANKL has been found to be involved in the control of body temperature [16], therefore it is now accepted that it has multifunctional roles in a variety of pathophysiological conditions. The extracellular active domain of RANKL can be enzymatically cleaved, affecting target cells in a paracrine fashion [17]. Therefore, it is a translational challenge to implement soluble (s)RANKL shedding in order to make its effects systemic.

A severe genetic pathology, known to depend on mutations of the *TNFSF11* gene encoding RANKL [18], belongs to the autosomal recessive osteopetrosis disease family, a bone disorder characterized by lack of osteoclast bone resorption [1] causing lethal skeletal, hematological and neuronal failures. Several subtypes of osteopetrosis are known, classified as osteoclast-rich and osteoclast-poor [19]. Osteoclast-rich osteopetroses present with fully differentiated but non-functional osteoclasts due to mutations of genes involved in the mechanism of bone resorption [19]. In osteoclast-poor osteopetroses, osteoclasts do not form because of loss-of-function mutations of genes involved in osteoclastogenesis, such as *TNFSF11*, encoding RANKL [18], and *TNFRSF11A*, encoding its receptor RANK [20]. While RANK is an osteoclast lineage intrinsic protein [21], RANKL ligand is expressed by other cell types [7,12,13,22], therefore osteopetrosis induced by its deficiency is not osteoclast-autonomous [18].

Osteoclasts belong to the myeloid lineage [23], therefore most forms of osteopetrosis are treated by hematopoietic stem cell transplantation, with increasing success of engraftments over the last decade even for mismatched donors [24]. Unfortunately, given that RANKL deficiency is caused by an osteoclast non-autonomous defect, this treatment regimen cannot be applied to this form of osteopetrosis and new therapies need to be developed.

Mouse models of RANKL deficiency were generated in 1999 and 2000 [25,26]. These models have been fully characterized and shown to respond to RANKL by a recovery of osteoclastogenesis [25]. Lo Iacono et al. [27] have recently demonstrated that infusion of RANKL could indeed partially rescue the osteopetrotic phenotype of RANKL-deficient mice and hypothesized that treatment of humans with the soluble cytokine could be feasible [1]. However, there are several pitfalls in this treatment regimen [1], including RANKL accumulation over time inducing severe overdose problems, which make it difficult to currently predict a translational impact of this study.

RANKL deficiency is a paradigm of a disease due to lack of a cytokine. Therefore, we believe that this model is ideal to investigate new biotechnological approaches to overcome, in the future, the above-mentioned pitfalls for the treatment of these types of diseases. However, before setting a specific translational protocol, we need a proof-of-principle that such an approach could work in an appropriate animal model. The *tnfsf11* knockout (KO) mice have the unique feature to generate no osteoclasts at all [25,26], therefore any positive effect induced by innovative methods of RANKL delivery could be easily validated by the appearance of cells of the osteoclast lineage, whose detection can straightforwardly be obtained by histochemical staining of the osteoclast-specific marker Tartrate-Resistant Acid Phosphatase (TRAcP) [28].

The prototype of our biotechnological device is the diffusion chamber, which is a well-established tool to study several in vivo biological processes, also in bone biology. It has largely been used in several studies to investigate in vivo osteoblast and osteoclast functions and regulation of bone formation and bone resorption [29,30]. Moreover, it is suitable for studies concerning bone tissue engineering [31], and for supplying hormonal factors to deficient backgrounds [32].

Diffusion chambers are made by overlapping plexiglas rings and porous durapore membranes (pore diameter 0.22 μm), that delimit an internal space in which cells grow. The durapore membranes provide high flow rates and throughput, low extractable and broad chemical compatibility. Cells are inoculated in the chamber and, through their pores, durapore membranes allow diffusion of water, solutes and macromolecules into the microenvironment, but prevent migration of cells outside the chamber, therefore, in vivo, cells do not interact with the host immune system and do not elicit cell-mediated immune response.

The aim of this study was to exploit the *tnfsf11* KO mice to test the principle that systemic delivery of a membrane-bound curative cytokine is feasible using diffusion chambers carrying RANKL-producing cells enzymatically manipulated to promote the active ectodomain shedding. In vivo implant of our diffusion chambers in *tnfsf11* KO mice demonstrated that, by our biotechnological approach, sRANKL can be released by cells into the circulation and induce systemic effects, as assessed by the appearance of functional osteoclasts in the bone of implanted mice.

2. Materials and methods

2.1. Animals

Procedures involving animal care were conducted in conformity with national and international laws and policies (EEC Council Directive 86/609, OJ L 358, 1, Dec. 12, 1987; Italian Legislative Decree (Gu n. 61, 14/03/2014); NIH guide for the Care and Use of Laboratory Animals, NIH Publication No. 85-23, 1985), and were approved by the Institutional Review Board of the University of L'Aquila. At the end of the experiments, mice were sacrificed by CO_2 inhalation. Wild type (WT) mice used for primary cell cultures were on CD1 background, while *tnfsf11* KO mice and their WT counterpart used for in vivo implants were on C57BL6/CD1 background.

2.2. Cell cultures

Mouse osteoblast cultures were derived from 8-to-10 day-old mice. Briefly, calvariae were dissected and sequentially digested with 1 mg/ml Clostridium histolyticum type IV collagenase (Sigma) and 0.025% trypsin (Becton Dickinson) in Hank's buffered solution. Cells from second and third digestions were grown in Dulbecco's modified Minimum Essential Medium (DMEM) with antibiotics and 10% Fetal Bovine Serum (FBS). At confluence, cells were released by trypsin procedure, counted and plated in appropriate vessels for further experiments. The osteoblast phenotype was evaluated by histochemical analysis of ALP activity, using reagents and protocols from the Sigma–Aldrich kit 104-LS. Mineralization assay was performed in osteoblasts cultured for 21 days in osteogenic medium [DMEM supplemented with FBS (10%), β-glycerophosphate (5 mM) and ascorbic acid (50 μg/ml)], and evidenced by alizarin red in 4% formalin-fixed cell cultures. When required, osteoblasts were treated with human recombinant ParaThyroid Hormone 1-34 [hrPTH(1-34)] (Sigma–Aldrich, cat # P3796).

Bone marrow stromal cells were the adherent cells after 48 h from flashing out and culturing the total bone marrow cells from long bones of 8-to-10 days old mice.

Bone marrow mesenchymal stem cells were obtained by immunomagnetic sorting of mouse bone marrow cells, using antibodies recognizing the specific markers STRO-1 and c-kit (Myilteny Biotech).

2.3. Cell culture support

Hydroxyapatite (HA) intact granulates and tridimensional (3D) HA scaffolds (Scaffdex CellCeram™) were purchased from Sigma Aldrich (cat # 289396 and cat # Z682012, respectively). They were used to culture primary osteoblasts obtained as described above, according to the manufacturer's instruction.

2.4. Diffusion chambers

Diffusion chamber kits (Millipore) were used for both in vitro and in vivo experiments, according to the manufacturer's instructions. They are made by two Plexiglas® Rings with 0.59 mm hole (Millipore cat # PR0001401) sealed using 13 mm durapore membrane filters, 0.22 micron pore size (Millipore cat # GSWP 013 00), glued altogether with Membrane Filter Cement (Millipore cat # XX70 000 72). Primary mouse calvarial osteoblasts were inoculated, with or without 3D HA, into the chambers, which were then sealed as described. For in vivo studies, the diffusion

chambers were implanted in the abdomen or in the flank of mice under deep anesthesia (2.5 mg Ketamine + 0.5 mg Xilazine in 100 μl saline solution/mouse).

2.5. sRANKL and osteoprotegerin (OPG)

sRANKL and OPG were quantified in cell conditioned media using the R&D System ELISA kits, MTR00 and MOP00 respectively, according to the manufacturer's instructions. Titration of free sRANKL was computed by the difference between equivalent weight of sRANKL and OPG obtained from ELISA, assuming 1:1 as reactive normality of sRANKL:OPG ratio.

Human recombinant sRANKL (Peprotech, cat # 310-01) was used for the in vitro osteoclastogenic assay.

2.6. Western blot and RT-PCR

For Western blots, reagents were from Sigma Aldrich. Conditioned media proteins resolved on a 12% SDS-PAGE were trans-blotted to nitrocellulose membranes and probed with the primary RANKL antibody (R&D, cat # AF462, 1:200) overnight at 4 °C, washed and incubated with the HRP-conjugated secondary antibody for 1 h at room temperature. Protein bands were revealed by enhanced chemiluminescence (ECL).

For Real-time RT-PCR, reagents were from Invitrogen. Total RNA was extracted using the Trizol®, then 1 μg was reverse transcribed and the equivalent of 0.1 μg was employed for the PCR reactions using the Brilliant® SYBR® Green QPCR master mix, using primer pairs specific for murine RANKL and OPG.

2.7. Enzymatic activity and immobilization

MMP14, MMP7 and TACE catalytic domains were purchased from Biomol. Catalytic activity was monitored by quenched fluorescent peptide substrate MCA (Biomol), according to the manufacturer's instructions. Immobilization procedures were performed with glutaraldehyde (10% v/v) (Sigma Aldrich).

2.8. Statistics

Data are expressed as mean ± standard deviation (s.d.). Statistical analysis was performed by the unpaired Student's *t* test or by the one-way Analysis of Variance (ANOVA). A p value <0.05 was considered statistically significant.

3. Results

3.1. Identification of cell type and culture condition to supply sRANKL

In the perspective of a translational application, one of the main strength of our approach could be the use of cells biologically expressing RANKL in a regulated fashion. This would offer the advantage of a "natural" control of the release of sRANKL which is not achievable using transfected cells or infusion of the cytokine. Therefore, the first part of the study had the aim to identify the best cell type and culture conditions to supply sRANKL.

To this purpose, we have tested mouse primary calvarial osteoblasts, bone marrow stromal cells and bone marrow mesenchymal stem cells. First, we evaluated different osteoblast densities to obtain both long-term survival and optimal sRANKL release in conditioned medium. We noted that the best cell density was 300,000 cells/cm^2, with which the evaluation of sRANKL by ELISA every five days showed a time-dependent free sRANKL accumulation in the culture medium (Fig. 1A). In the same culture conditions, bone marrow stromal cells showed lower release of sRANKL than osteoblasts (Fig. 1B). In addition, the assessment of cell viability demonstrated reduced cell survival with time. Therefore, we

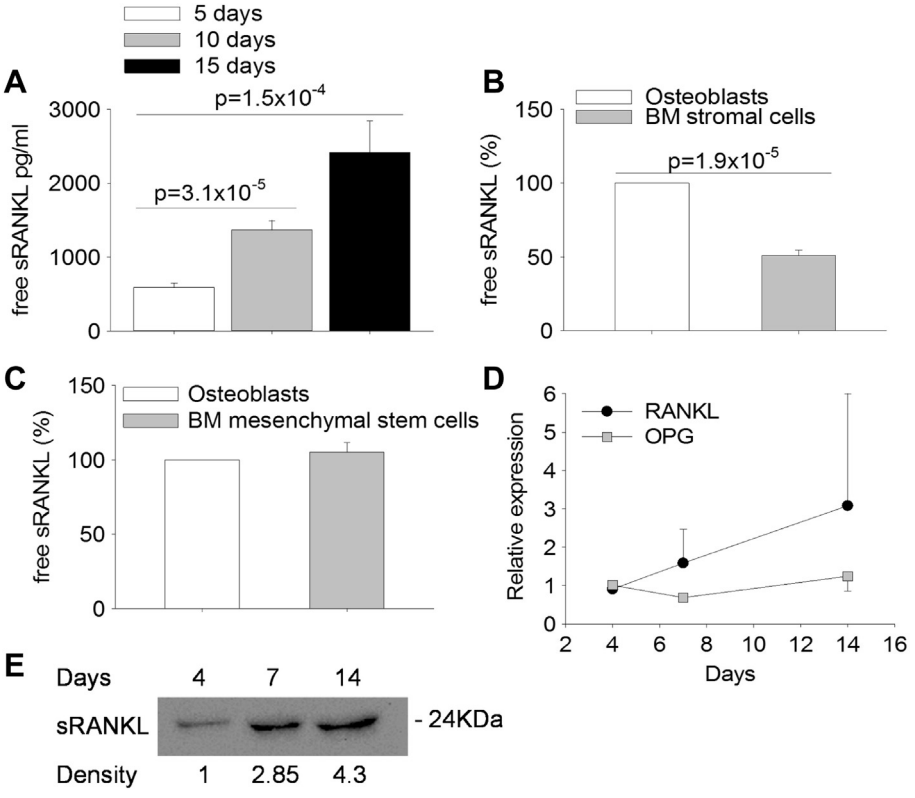

Fig. 1. Release of sRANKL in conditioned media. (A) ELISA assays were performed to evaluate the concentrations of sRANKL and of the RANKL-decoy receptor osteoprotegerin in conditioned media from osteoblasts cultured for the indicated times, then the free sRANKL concentration was calculated on the basis of a RANKL/OPG 1:1 M ratio. (B, C) ELISA assays as described in (A) to calculate the free sRANKL concentration in conditioned media from (B) mouse bone marrow (BM) stromal cells and (C) mouse BM mesenchymal stem cells, cultured for 5 days, in comparison with mouse calvarial osteoblasts. (D) Real-time RT-PCR on RNA extracted from primary osteoblast cultures at the indicated times of culture. (E) Western blot analysis of sRANKL released in the osteoblast conditioned media pooled at the indicated times of culture. Numbers below the bands represent the relative arbitrary densitometric units. Data are the mean ± s.d. of three independent experiments. Statistics: unpaired Student's *t* test.

concluded that this cell type is not suitable for our research. We then evaluated bone marrow mesenchymal stem cells. As shown in Fig. 1C, the sRANKL yield in these cultures was comparable to that of osteoblasts. We also isolated primary osteocytes which are considered the bone cells with the highest RANKL expression [33]. However, isolation procedure was time-consuming and proliferation rate of these cells in culture was low, making them unsuitable for a large-scale use. Therefore, because calvarial osteoblasts were more readily available and easy to handle, we considered them as the best biological sRANKL source suitable for our purpose. RT-PCR and Western blot analyses confirmed that these cells expressed RANKL and OPG mRNAs (Fig. 1D) and released sRANKL into the medium (Fig. 1E), therefore we decided to use them for improving sRANKL shedding.

3.2. Osteoblast cultures on hydroxyapatite supports

We evaluated sRANKL shedding in mouse primary calvarial osteoblasts grown on biocompatible supports. The purpose was to maintain cells in a situation closer to their in vivo setting and provide a substrate compatible with their long-term survival and enzymatic manipulation (see below). We used both granular hydroxyapatite (HA) and 3D HA scaffolds (Fig. 2A–D). Evaluation of conditioned media showed a higher spontaneous sRANKL release by osteoblasts cultured on HA supports than by cells grown on plastic dishes, with the 3D HA scaffolds better performing compared to the other conditions (Fig. 2E).

3.3. Regulated expression of RANKL

Since in vivo RANKL production is regulated by PTH, which is elevated in osteopetrosis, we assessed whether in our experimental conditions this hormone could improve the rate of sRANKL released by the osteoblasts. Consistent with this knowledge, we observed that treatment of our cell cultures with 10^{-8} M human recombinant (hr)PTH(1-34) increased the free sRANKL concentration by ~2.5 fold compared to basal conditions (Fig. 2F), suggesting that in vivo the hormone could regulate the yield of sRANKL from the implanted cells. Taken together, these results demonstrate that we have obtained a suitable cell source of sRANKL which can be used for our biotechnological approach in a manner physiologically regulated by hormonal factors, such as the PTH.

3.4. Enhancement of sRANKL shedding by enzymatic manipulation

Since cells retain RANKL in large part as membrane-bound protein, this could represent an important drawback in our

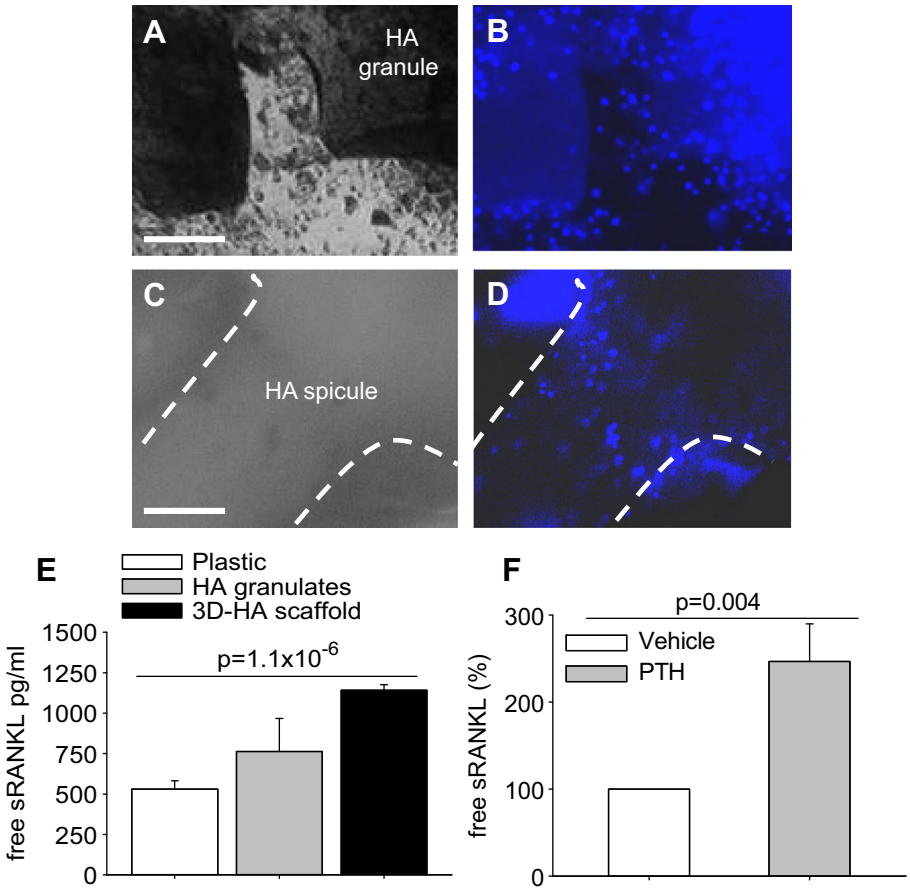

Fig. 2. Culture conditions and RANKL assays. (A) Phase contrast microscopy of mouse calvarial osteoblasts cultured on hydroxyapatite (HA) granulates for 5 days (Bar = 1 mm). (B) Nuclear staining by Hoechst dye (blue) of the same field as in (A) to identify the cells. (C) Phase contrast microscopy of mouse calvarial osteoblasts cultured on 3D HA scaffolds for 5 days (Bar = 1 mm). (D) Nuclear staining by Hoechst dye of the same field as in (C) to identify the cells. Dot line: edge of a HA spicule of the scaffold. (E) ELISA assays as described in Fig. 1A to calculate the free sRANKL concentration in conditioned media from osteoblasts grown on HA granulates or 3D HA scaffold for 5 days, compared to standard cultures on plastic dishes. (F) Mouse calvarial osteoblasts were cultured for 5 days in standard condition in the presence of vehicle or 10^{-8} M hrPTH(1-34), given every day for the timeframe of the experiment. ELISA assays as described in Fig. 1A to calculate the free sRANKL concentration in conditioned media. Data are (A–D) representative or (E, F) the mean ± s.d. of three independent experiments. Statistics: unpaired Student's *t* test.

translational application, which instead requires systemic delivery. Enzymatic ectodomain shedding induces the release of the active extracellular domain of membrane-bound cytokines, which become soluble and can circulate. MMP14 is a metalloproteinase known to have RANKL ectodomain shedding properties [34]. It is commercially available as active catalytic domain corresponding to the naturally-occurring active form of MMP14 which lacks the C-terminal hemopexin domain [35]. To initially test whether proteolytic shedding of sRANKL is feasible, we treated mouse primary calvarial osteoblasts with vehicle or with 50–1000 ng/ml MMP14 for 5 days. Morphological analysis of cell cultures showed normal cell viability and slight concentration-dependent decrease of Alkaline Phosphatase (ALP) histochemical activity by treatment with MMP14 (Fig. 3A). ELISA assay demonstrated a concentration-dependent increase of free sRANKL in conditioned media from cells treated with MMP14 versus control cultures (Fig. 3B). Furthermore, MMP14 did not impair osteoblast activity as demonstrated by normal mineralization of extracellular matrix nodules (Fig. 3C). Taken together, these results suggest that treatment with MMP14 is safe and effective in shedding sRANKL from its membrane-bound form even in long-term treatments.

Nevertheless, for our application, it is imperative to demonstrate that the enzyme could remain stable in long-terms, to allow its use also in in vivo experiments. To this aim we evaluated MMP14 catalytic activity using the fluorescent substrate (7-Methoxycoumarin -4-yl) acetyl-Pro-Leu-Gly-Leu-[3-(2,4-dinitrofenil)-L-2,3-diamino proprionyl]-Ala-Arg-NH_2 (MCA), keeping the enzyme at 37 °C and 5% CO_2 atmosphere for 15 days. The results showed that in the timeframe of our experiment, the enzyme retained its catalytic ability intact (Fig. 3D).

Other proteolytic enzymes, including MMP7 [36] and TNF-α Converting Enzyme (TACE) [37] also display RANKL shedding

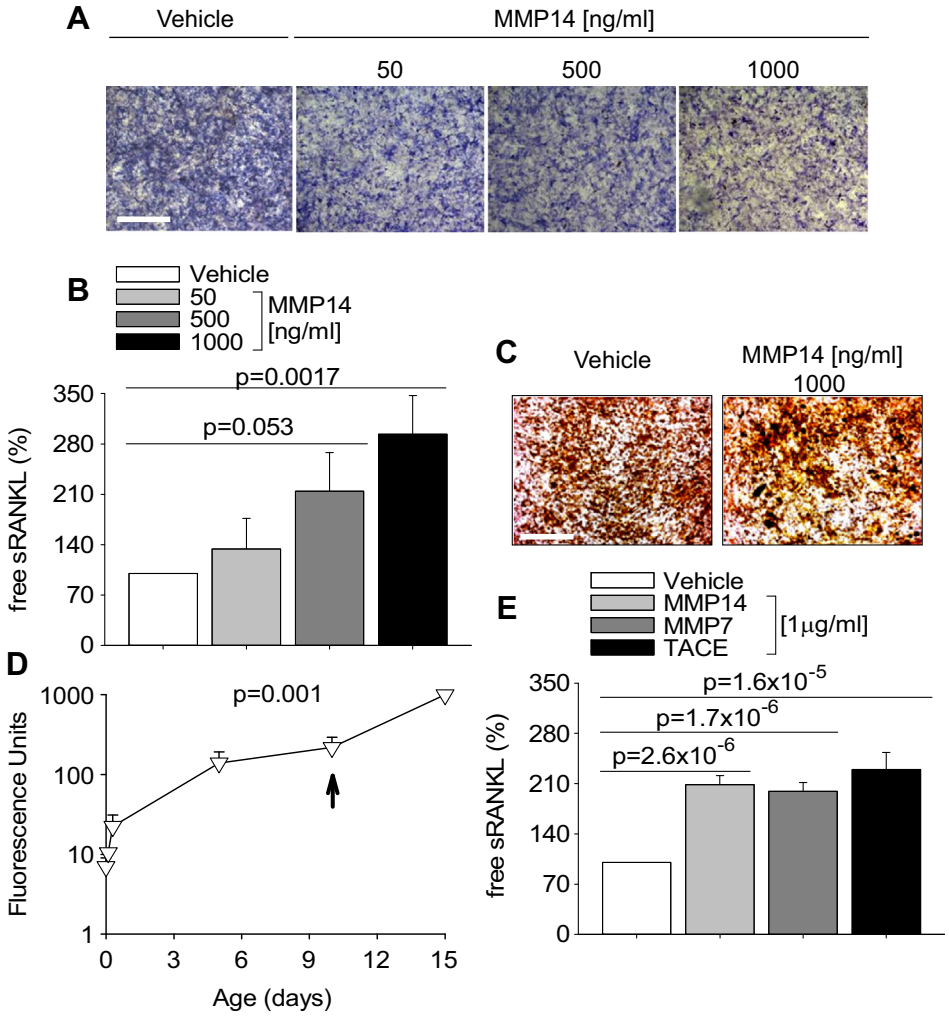

Fig. 3. Enzymatic treatments. (A) Histochemical evaluation of alkaline phosphatase cytochemical positivity (blue staining) in mouse calvarial osteoblasts treated with the indicated MMP14 concentrations for 5 days (Bar = 1 mm). (B) ELISA assays as described in Fig. 1A to calculate the free sRANKL concentration in conditioned media from cells treated as described in (A). (C) Mineralization assay by alizarin red in mouse calvarial osteoblasts cultured in osteogenic medium treated with the indicated MMP14 concentration for 5 days (Bar = 1 mm). (D) Stability of the catalytic activity of 50 ng/ml MMP14 analyzed in cell-free condition, in a long-term time-course experiment of degradation of quenched fluorescent peptide 7-methoxycoumarin-4-yl)acetyl-Pro-Leu-Gly-Leu-[3(2,4-dinitrophenyl)-L-2,3-diaminopropionyl]-Ala-Arh-NH_2 (MCA). Peptide substrate was added at time 0 at concentration of 1 μM, then accumulation of the fluorescent product was analyzed up to day 10, when a plateau was reached. At this time, excess peptide substrate (20 μM) was added and reaction proceeded up to day 15. Results are the mean ± s.d. of a triplicate experiment. (E) Mouse calvarial osteoblasts were cultured for 5 days with 1 μg/ml of the indicated enzymes, then ELISA assays were performed as described in Fig. 1A to calculate the free sRANKL concentration in conditioned media. Data are (A, C) representative or (B, D, E) the mean ± s.d. of three independent experiments. Statistics: (B, E), unpaired Student's *t* test; (D), one-way ANOVA. (For interpretation of the references to colour in this figure legend, the reader is referred to the web version of this article.)

activity. Hence, we next tested whether there could be any advantage in using these two enzymes instead of MMP14. Fig. 3E shows that MMP14, MMP7 and TACE had similar RANKL shedding activity. Thus, we decided to keep with MMP14.

3.5. MMP14 immobilization

To the purpose of our study, in vivo systemic effects of the MMP14 are not desirable as it could affect various biological pathways if released into the circulation. To sort out this problem, we tested the possibility to immobilize the recombinant catalytic domain of MMP14 on substrate, which will locally subject the cells to the continuous action of the enzyme, preventing its egress into the circulation. For the first evaluation, we absorbed MMP14 on Glutatione-S-Transferase (GST)-agarose beads using glutaraldehyde. This aldehyde has the ability to form covalent bonds between two molecules, interacting with the hydroxylic groups of serine/tyrosine and causing molecule immobilization on substrate [38]. Assessment of degradation of the fluorescent peptide MCA showed that in this condition the catalytic activity was low (Fig. 4A). We hypothesized that this inconvenience could arise from chemical alteration of the enzyme catalytic site caused by glutaraldehyde cross-links. We therefore decided to protect this site by pre-incubation for 2 h with MCA (20 and 50 μM), namely the same substrate used for determining the MMP14 catalytic activity. We then washed out the MCA and incubated again the GST-agarose bead-immobilized enzyme with MCA for re-testing the hydrolytic activity. We observed that indeed this pre-incubation with MCA was effective, resulting in a concentration-dependent protection capacity of the substrate (Fig. 4A).

3.6. Enzymatic shedding of sRANKL from cells cultured on 3D HA scaffolds

To exploit the sRANKL shedding ability of MMP14, we engineered the 3D HA scaffolds with MMP14, using the glutaraldehyde treatment. We used different combinations of glutaraldehyde (10–20%) and MCA (1–2 μg/ml), in order to improve the immobilization efficiency. These combinations were successful but we were unable to obtain an enzymatic efficiency of functionalized scaffolds greater than ~50% compared to soluble MMP14 (Fig. 4B).

We therefore decided to test whether even 50% preserved catalytic activity could suffice to increase sRANKL release from cells. We cultured mouse calvarial osteoblasts on 3D HA scaffolds

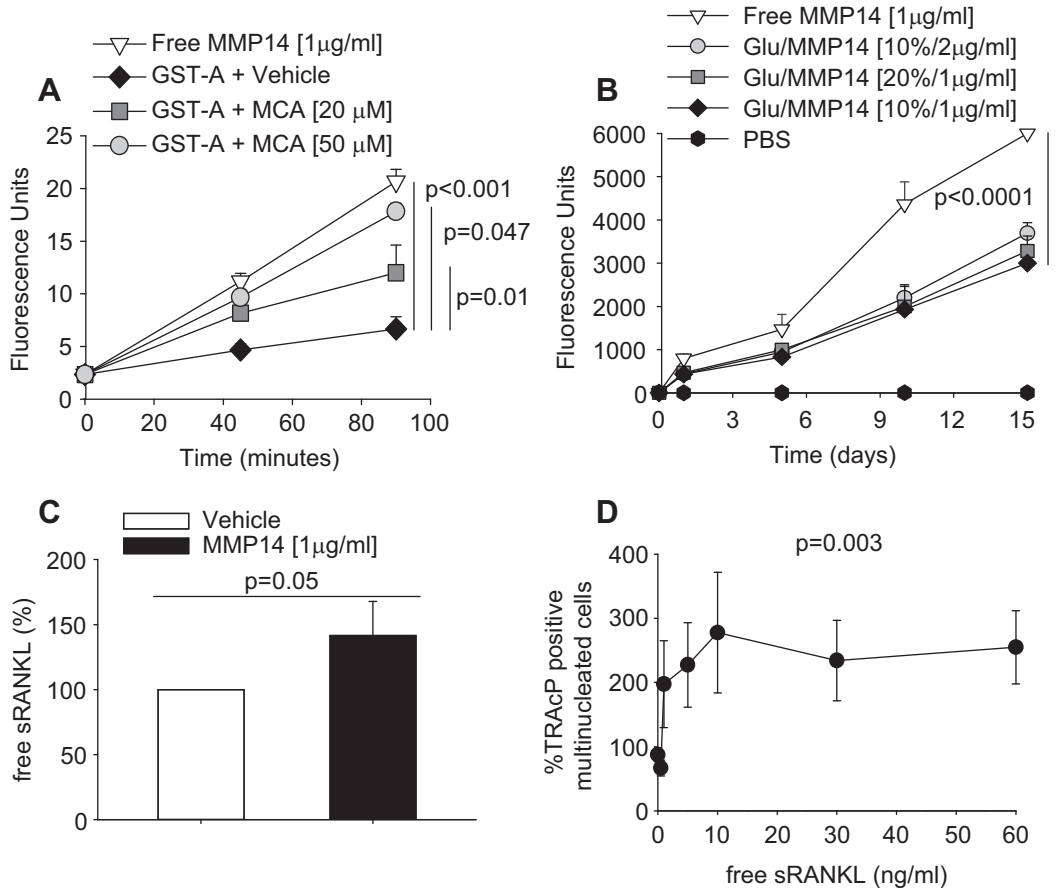

Fig. 4. MMP14 immobilization and osteoclastogenesis assay. (A) MMP14 (1 μg/ml) was adsorbed to GST-agarose (GST-A) beads by overnight incubation at 37 °C with 2.5% of the cross-linker agent glutaraldehyde. The catalytic activity of absorbed MMP14 was protected by pre-incubation for 2 h with 20 or 50 μM MCA. MMP14-adsorbed GST-agarose beads were then extensively washed to remove both MCA and glutaraldehyde, and incubated with 1 μM MCA for the indicated times at 37 °C. Free (non-adsorbed) MMP14 was used as positive control. (B) Immobilization of MMP14 on 3D HA scaffold, using different concentrations of both glutaraldehyde (Glu) and MMP14, as indicated. Procedures for immobilization were the same described in (A). Free (non-adsorbed) MMP14 was used as positive control. Phosphate Buffer Saline (PBS) was used as negative control. (C) ELISA assay as described in Fig. 1A to calculate the free sRANKL concentration in conditioned media from mouse calvarial osteoblasts cultured on 3D HA scaffold functionalized with vehicle or with MMP14 as indicated. (D) Ficoll-purified mouse bone marrow osteoclast precursors were incubated for 6 days with 10 ng/ml M-CSF and the indicated concentrations of human recombinant RANKL. At the end of incubation, cells were fixed and stained for the osteoclast-specific marker Tartrate-Resistant Acid Phosphatase (TRAcP). Multinuclear (>3 nuclei) TRAcP-positive cells were then enumerated and expressed as % of untreated cultures. Average numbers at plateau ranged between 15 and 40 osteoclasts/well (96 multiwell plates). Data are expressed as the mean ± s.d. of three independent experiments. Statistics: (A, B, D), one-way ANOVA; (C), unpaired Student's *t* test.

functionalized with MMP14 as described above. ELISA evaluation of conditioned media showed that the yield of sRANKL from osteoblasts cultured on MMP14-functionalized scaffold was higher than in conditioned media from osteoblasts cultured on intact scaffold (Fig. 4C), confirming that MMP14 was correctly immobilized and effective in shedding the RANKL active domain from the membrane bound RANKL. We evaluated this enzymatic ability up to 30 days of culture and observed that it was maintained intact for the timeframe of this observation.

3.7. Osteoclastogenesis assay

The average concentration of sRANKL achieved in these experimental conditions at 5 days of culture was greater than 2 ng/ml. To verify whether this concentration was suitable to enhance osteoclast formation, we performed an osteoclastogenesis assay in the presence of increasing concentrations of commercially available sRANKL. In our culture conditions, we observed that 1 ng/ml sRANKL induced osteoclast formation near the plateau level (Fig. 4D), suggesting that with our strategy we achieved sRANKL levels sufficient to support osteoclast formation in vitro.

3.8. In vivo implants

To assess the feasibility of our strategy in vivo, we first performed preliminary tests to set up the conditions to implant the diffusion chambers in mice. We implanted diffusion chambers containing 1,000,000 mouse primary calvarial osteoblasts/chamber without scaffold, subcutaneously, in the abdomen of 30-days old wild-type (WT) C57BL6 mice and monitored animals for 3 weeks. In this timeframe, we did not observe any sign of distress. We euthanized the mice and gathered the diffusion chambers. We did not observe obvious internal damages or signs of inflammation at autopsy near the area of implant. Diffusion chambers contained viable cells, which resulted positive to the osteoblast marker, ALP (Fig. 5A).

We then tested the implant of diffusion chambers containing MMP14-functionalised scaffold harboring osteoblasts in younger WT C57BL6 mice (10–20 days of age). We made this choice in order to verify that no damage occurred due to the presence of the scaffold in the diffusion chamber, and to set up the implant procedure as early as possible. We observed that the hold of the diffusion chambers in mice younger than 21 days was problematic due to skin damage at the implant site. However, in mice in which the diffusion chambers were successfully engrafted, after 3 weeks from implant they contained viable cells on scaffold. These results warn about the age of animals to be implanted, but confirm that the scaffold and its enzymatic functionalization by MMP14 causes no harm.

Having established that implanted mice cannot be younger than 21 days, we tested *tnfsf11* KO mice at this age, implanting them with diffusion chambers containing MMP14 functionalized scaffold harboring osteoblasts. Unfortunately, due to their body size much lower than the WT counterpart, only some *tnfsf11* KO mice succeeded to retain the diffusion chambers. At the end of the experiment, their body weight was similar to that of the control *tnfsf11* KO

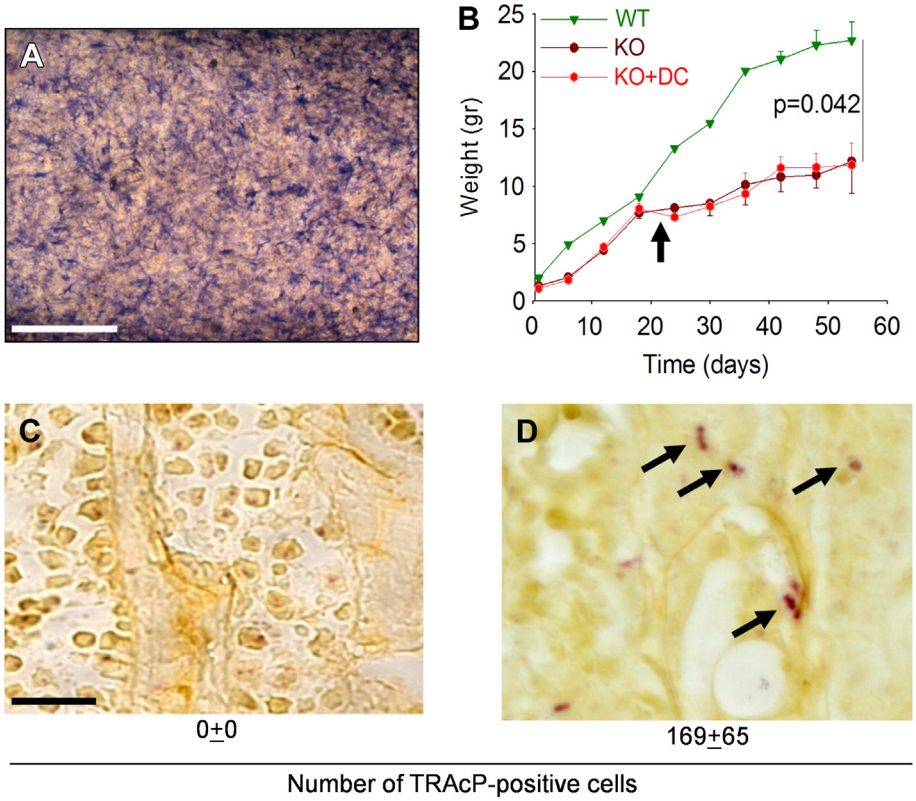

Fig. 5. In vivo implants of Diffusion Chambers (DC) in young *tnfsf11* knockout (KO) mice. (A) DCs containing primary calvarial osteoblasts implanted in a 1 month-old WT mice and harvested after 3 weeks. Cytochemical staining for the osteoblast-specific marker alkaline phosphatase (Bar = 1 mm). (B) Body weight expressed in grams (gr) of wild type (WT) and *tnfsf11* knockout mice treated with PBS (KO) or implanted at the age of 21 days (arrow) with one DC containing primary calvarial osteoblasts on MMP14-functionalized 3D HA scaffold (KO + DC). (C, D) Histological sections of proximal tibia histochemically stained for the Tartrate-Resistant Acid Phosphatase (TRAcP), showing (C) no TRAcP-positive cells in a non-implanted KO mouse and (D) small TRAcP-positive cells (arrows) in a KO mouse implanted for 1 month with a DC containing primary calvarial osteoblasts on functionalized 3D HA scaffold (Bar = 50 μm). Results are representative (A, C, D) or (B) the mean ± s.d or three mice per group. Statistics: one-way ANOVA. (For interpretation of the references to colour in this figure legend, the reader is referred to the web version of this article.)

mice (Fig. 5B). However, the implanted mice were more active and lively while the untreated *tnfsf11* KO counterparts were generally apathetic. Mice were euthanized between 15 and 30 days from the implants (age 36–51 days) and long bones were histochemically evaluated for the osteoclast-specific enzyme TRAcP. We noticed the presence of small TRAcP-positive cells, presumably mononuclear precursors belonging to the osteoclast lineage, in tibias of all animals of the implanted group. TRAcP staining was instead totally absent in all control animals histologically evaluated in the study (Fig. 5C,D). Furthermore, in some *tnfsf11* KO animals of this group we experienced again the loss of diffusion chambers between 3 and 14 days from surgery. Therefore, the success of retaining of the implant in the abdomen of 21 days-old *tnfsf11* KO mice was still problematic.

To overcome this problem we grew the *tnfsf11* KO mice to adulthood through the administration of a soft diet, which prevented the insufficient nutrition due to the lack of tooth eruption [25,26]. This allowed us to implant *tnfsf11* KO mice with 1 diffusion chamber between 36 and 42 days of life. Mice did not show any distress due to the implant. However, they did not exhibit

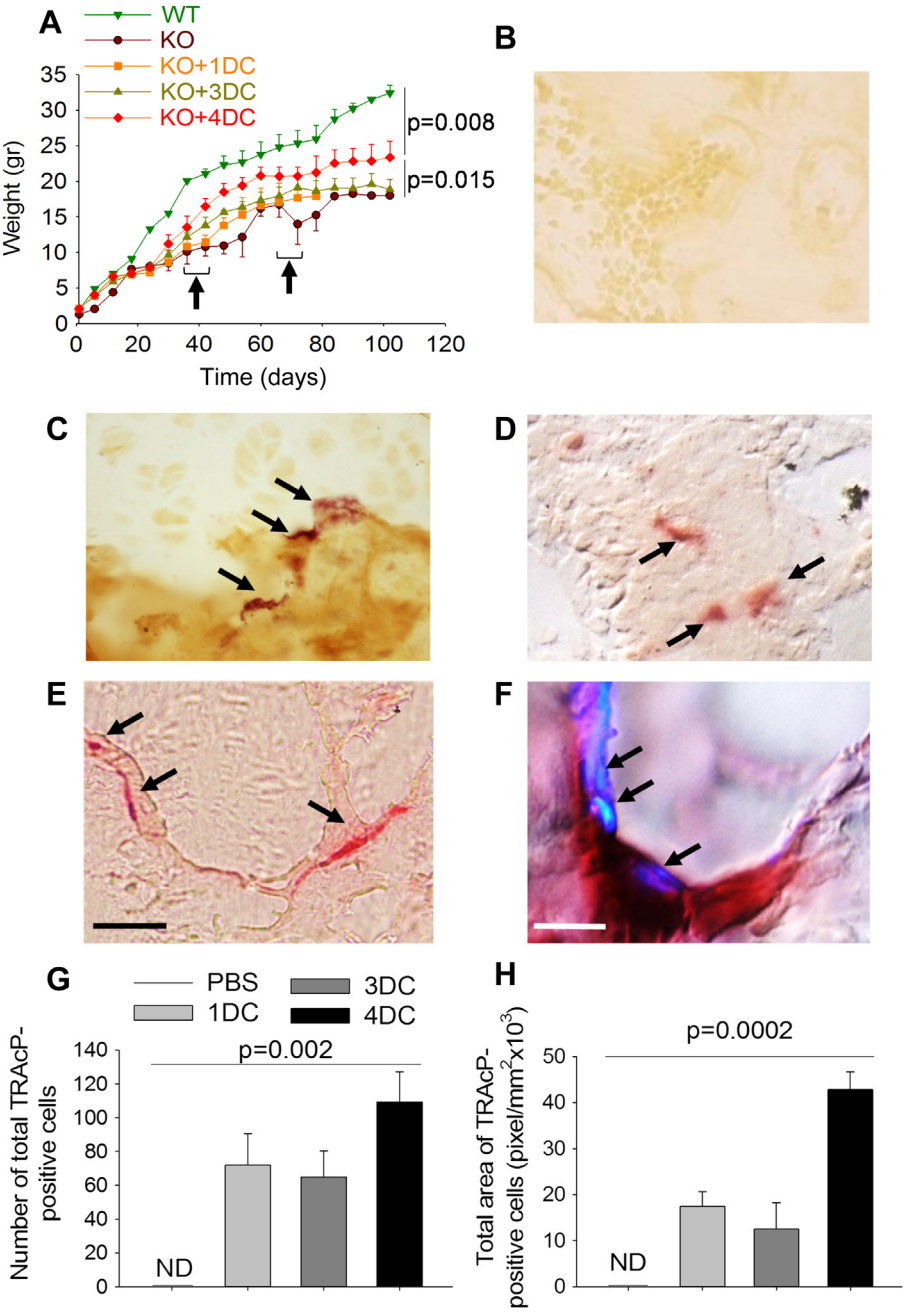

Fig. 6. In vivo implant of Diffusion Chambers (DC) in adult *tnfsf11* knockout (KO) mice. Body weight expressed in grams (gr) of wild type (WT) mice and *tnfsf11* knockout mice treated with PBS (KO) or implanted with 1 (KO + 1DC), 3 (KO + 3DC) or 4 (KO + 4DC) diffusion chambers containing primary calvarial osteoblasts on MMP14-functionalized 3D HA scaffold. Arrows: time of first (1 or 2 DC) and second (2 DC) implants (B–E) Histological sections of proximal tibias histochemically stained for the Tartrate-Resistant Acid Phosphatase (TRAcP) (arrows) showing TRAcP-positive cells in KO mice implanted with (C) 1, (D) 3 and (E) 4 DCs (Bar = 50 μm). (F) High magnification of a TRAcP-positive osteoclast sitting on bone in histological section of proximal tibia of a KO mouse implanted with 4 DCs in which nuclei (arrows) have been stained with DAPI (Bar = 10 μm). (G) Quantification of the number of osteoclasts/tibia. (H) Quantification of the mean osteoclast area. Results are (B–F) representative or (A, G, H) the mean ± s.d of three mice per group. Statistics: (A) one-way ANOVA; (G, H) unpaired Student's *t* test).

increase of their weight compared to control mice (Fig. 6A). They were sacrificed after one month from implant. Notably, histochemical evaluation of tibias confirmed the appearance of TRAcP-positive cells in the implanted mice compared to controls (Fig. 6B,C).

In further groups of *tnfsf11* KO we implanted 1 or 2 diffusion chambers at 36 days of life. After 1 month (age 72 days) they were replaced with two fresh diffusion chambers and mice were sacrificed 1 month later (age 102 days). While mice implanted with total 3 diffusion chambers still did not show any growth improvement, those implanted with 4 diffusion chambers exhibited an increase of body weight. Moreover, in histological sections, we observed TRAcP-positive cells (Fig. 6D,E) that, in the group implanted with 4 diffusion chambers, adhered to the bone surface and were morphologically very similar to mature osteoclasts (Fig. 6E). In addition, histochemical staining for TRAcP and nuclear co-staining with DAPI, unraveled that these cells were multinucleated (Fig. 6F). These data were confirmed quantitatively. In fact, in the group implanted with 4 diffusion chambers we observed a higher number of TRAcP-positive cells (Fig. 6G) and a greater TRAcP-positive cell area (Fig. 6H), suggesting that, with this strategy, we obtained full osteoclastogenesis.

Next, we assessed in histological sections whether the newly formed osteoclasts were functional. To this end, we measured the eroded bone surface underneath the TRAcP-positive cells and observed that, at variance with non-implanted *tnfsf11* KO mice, in which there were no osteoclasts and eroded surface, in the 4 diffusion chambers implanted mice eroded surface underneath the TRAcP-positive multinuclear cells was quantifiable (Fig. 7A). Finally, to assess whether this level of bone resorption could induce any benefit on the structure of the bone, we measured the proximal tibia trabecular bone volume over total tissue volume and observed a significant decrease compared to the non-implanted *tnfsf11* KO mice (Fig. 7B). Taken together, these results demonstrated that with the implant of 4 diffusion chambers total, we obtained functional osteoclasts capable of eroding the bone surface and reduce the trabecular bone mass in tibias.

Finally, to assess whether our strategy could induce adverse effects, we performed histological evaluation of lungs, which were reported to undergo worsening of lymphoid infiltrations in *tnfsf11* KO mice treated with sRANKL [27]. Our analysis demonstrated no changes in number and size of lymphoid aggregates in implanted KO mice compared to their non-implanted counterpart (Fig. 8), suggesting that at least this variable is not aggravated by our treatment.

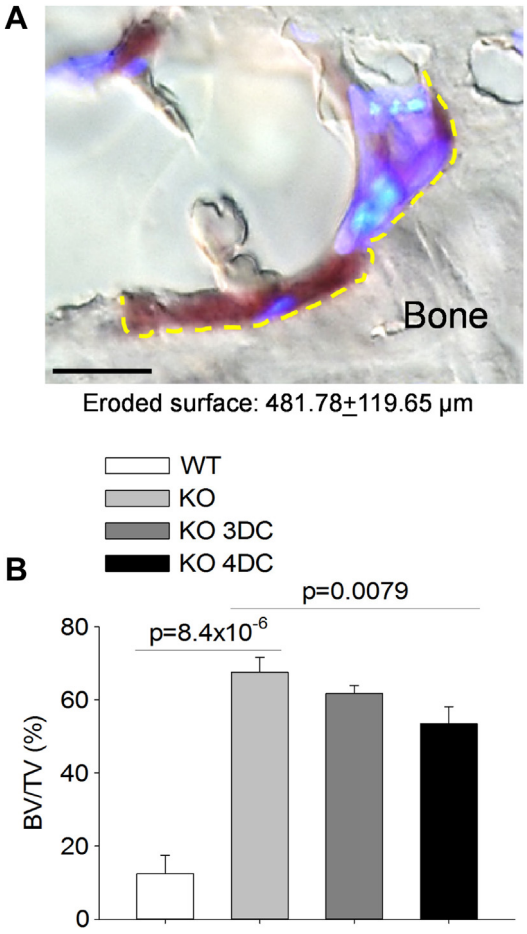

Fig. 7. Bone resorption and trabecular bone structural variable in *tnfsf11* knockout (KO) mice implanted with Diffusion Chambers (DC). (A) Representative osteoclast of a KO mouse implanted with 4 DCs showing Tartrate-Resistant Acid Phosphatase (TRAcP)-positivity (purple staining), multinuclearity (DAPI blue staining) and ability to excavate Howship lacuna (yellow dotted line) (Bar = 10 µm). (B) Quantification of the trabecular bone volume over the total tissue volume (BV/TV) in proximal tibias of WT and KO mice treated with PBS or implanted with 3 or 4 DCs. Results are (A) representative or (B) the mean ± s.d of 3 mice per group. Statistics: unpaired Student's *t* test.

4. Discussion

In this study, we were able to demonstrate that a biotechnological approach allows the release of the active ectodomain of membrane-bound RANKL from mouse primary calvarial osteoblasts in an amount that induced the formation of functional osteoclasts. We showed that, among the RANKL cell sources tested, calvarial osteoblasts were the most efficient and easy to handle. Bone marrow stromal cells produced about half of the sRANKL amount produced by osteoblasts, while bone marrow mesenchymal stem cells, although as efficient as osteoblasts in sRANKL yield, required time and effort to be isolated. Likewise, osteocytes needed time-consuming isolation procedures and showed low yield and slow proliferation rate in culture, therefore, although they are great RANKL producers [33], they are currently not suitable for biotechnological purposes.

We also demonstrated that substrate and culture conditions are important factors to improve the yield of sRANKL. In fact, HA supports were more efficient than plastic dishes to stimulate cytokine release by osteoblasts, and 3D cultures on HA scaffolds were more efficient than 2D cultures on HA granulate. HA is a natural substrate for osteoblasts that could contribute to create a more physiologic environment. In addition, in vivo osteoblasts sit on 3D bone structures, therefore, not surprisingly, the 3D HA scaffolds supported the best yield of sRANKL, that was double compared to osteoblasts cultured on plastic, and 1.5 fold more than in osteoblasts cultured on HA granulate. This was a fortunate circumstance because it allowed us to immobilize a RANKL-shedding enzyme on 3D scaffolds and improve the efficiency of sRANKL discharge in the conditioned medium.

In fact, the active domain of RANKL is displayed extracellularly and, in certain circumstances, it can be released in the microenvironment through enzymatic cleavage [39]. RANKL deficiency induces a systemic disease, which cannot be cured by local procedures. Major effects of RANKL in bone are exerted in a paracrine manner, and the bound of the cytokine to the osteoblast plasma membrane ensures a controlled regulatory activity on osteoclast precursors through cell-to-cell contact [40]. Unfortunately, this physiologic circumstance limits the use of cell implants when a membrane-bound cytokine is desirable to exert systemic effects. We overwhelmed this inconvenience testing various

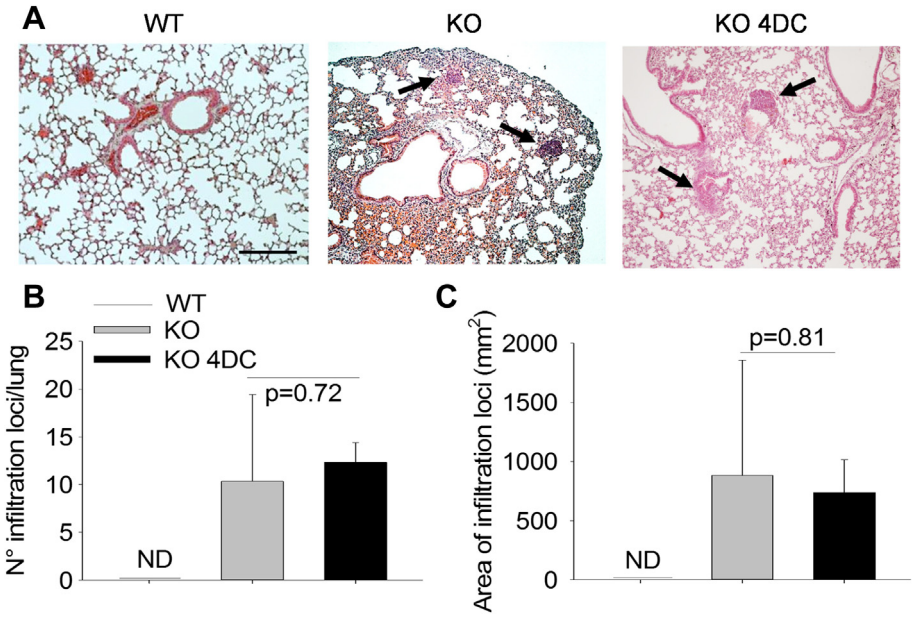

Fig. 8. Lymphoid aggregates in lungs. (A) Histological sections of lungs from WT and *tnfsf11* knockout mice untreated (KO) or subjected to implants of 4 DC total (KO 4DC), stained with hematoxylin/eosin, showing lymphoid aggregates (arrows). (Bar = 100 μm). (B, C) Quantification of (B) number and (C) area of lymphoid aggregates in lungs. Results are (A) representative or (B, C) the mean ± s.d of 3 mice per group. Statistics: unpaired Student's *t* test. (For interpretation of the references to colour in this figure legend, the reader is referred to the web version of this article.)

RANKL-shedding enzymes, MMP14 [34], MMP7 [36] and TACE [37], which were equally efficient in releasing the RANKL ectodomain in the conditioned medium. We focused on MMP14 and were able to immobilize its commercially available catalytic domain on the 3D HA scaffolds. The MMP14 enzymatic activity was stable over time and enabled a significant enhancement of sRANKL shedding compared to intact scaffolds. Altogether, these maneuvers resulted in a sRANKL yield sufficient to induce osteoclastogenesis in vitro and in vivo.

To investigate the impact of our biotechnological device in vivo, we took advantage of the *tnfsf11* KO mouse model that is characterized by the total absence of the osteoclast lineage and by complete TRAcP negativity in histological sections. We observed that diffusion chambers, inoculated with osteoblasts on MMP14-engineered 3D HA scaffolds and implanted in vivo in *tnfsf11* KO mice, were able to support long-term osteoblast survival and to induce TRAcP activity in tibia sections, suggesting that our sRANKL could enter the circulation and reach the skeleton. In our best implant conditions, we also observed an increase of *tnfsf11* KO mouse body weight over untreated controls, suggesting an improvement of somatic growth. Control *tnfsf11* KO mice were instead completely negative to the histochemical detection of TRAcP, showed severe growth retardation and, with a few exceptions, died within the 50th day of life. Most interestingly, in our experimental conditions, we noted the appearance of TRAcP-positive cells on bone surface morphologically and functionally resembling mature osteoclasts. We believe that these results provide a strong background for future studies aimed at addressing the curative effect of the in vivo implants of RANKL-producing cells into a RANKL-deficient mouse model.

Compared to other experimental therapies, our proposed approach could have several advantages. It could replace pharmacological treatments that over time could cause problems of compliance. In fact, since RANKL is a protein, only parenteral administration can be foreseen for this type of therapy, which for chronic administrations is known to be poorly tolerated by patients. Another problem with the pharmacological treatment is the dosage. Administration of 1 mg/kg sRANKL every 2 days for 5 weeks has already been implemented in RANKL KO mice [27], with good responses and phenotypic improvements, but with incomplete disease rescue. Mice still showed growth retardation and partial recovery of hypocalcemia, while tooth eruption and lymph node genesis remained impaired. Furthermore, in this study, sRANKL overdose was experienced after 3 months of treatment. In fact, while growth retardation, tooth eruption and lymph node genesis were not improved, bone mass was severely decreased below the levels of the wild type littermates, inducing an osteopenic phenotype. Moreover, overstimulation of developing T-cells was observed that could potentially induce self-reactive clones escaping the selection process. Large lymphoid aggregates appeared in lungs and gut, along with hepatization of the lung parenchyma. Lungs presented extensive exudates and their function was severely impaired, probably representing the cause of death of some mice. Consistently, treatment with 2 mg/kg sRANKL resulted in a potent toxic effect, with even larger lymphoid expansion in lungs and death occurring at the 2nd week of treatment. Based on these results, we believe that a biotechnological device containing sRANKL cell sources regulated physiologically, as demonstrated in this study for instance by PTH, could bypass the overdose problems and be more tolerated in long-term treatments. In fact, PTH, which is elevated in osteopetrosis due to the hypocalcemic condition [41,42], could play a central role in the control of RANKL expression in osteoblasts implanted in vivo for therapeutic purposes. It could induce a burst of sRANKL release in the first phase of treatment then, being attenuated by the stabilization of calcemia, it could contribute to a more physiologic release of the cytokine according to the calcemic status of the subject.

The use of diffusion chambers that isolate the implanted cells from the host tissue could represent another advantage compared to traditional cell implants. In fact, while consenting the flow of soluble factors, the durapore membrane prevents the contact of the implanted cells with the host tissue. Although T lymphogenesis is impaired in RANKL KO mice, the reaction to allografts has not been evaluated and it could be a prudent maneuver to isolate implanted

cells from the host immune system. Of course, immune response could still occur against the cytokine itself. However, this would be a problem also for pharmacological therapy or for conventional cell transplantation. In the case of RANKL, however, we predict that this is likely not to occur due to the fact that both the animal model of RANKL deficiency [25,26] and patients affected by mutations of the *TNFSF11* gene [18] carry non-functional proteins which could induce immune tolerance, thus preventing immune response to the exogenous intact RANKL.

Finally, we believe that our strategy could be applied also beyond osteopetrosis. In fact, similar devices could be employed for deficiencies of other cytokines. In this case, the prevention of the immune response by isolating the curative cells from the host tissue could be even more important if the disease did not show immune failure.

5. Conclusions

In this work, we have provided the proof-of-principle that diffusion chambers could be used to induce active ectodomain shedding of a membrane-bound cytokine. Indeed, we have demonstrated that the osteoclastogenic cytokine, RANKL, was released by osteoblasts, and that appropriate culture conditions, osteoblast adhesion to 3D HA scaffold and functionalization of scaffold with MMP14 enhanced its shedding making it measurable in conditioned media to a concentration compatible with the induction of osteoclastogenesis. We also demonstrated that, in vivo, sRANKL released through the permeant diffusion chambers entered the circulation and triggered systemic effects, inducing osteoclastogenesis and improving the bone phenotype of *tnfsf11* KO mice. Considering the overdose adverse effects demonstrated for the administration of sRANKL in *tnfsf11* KO mice [27], we believe that our approach could tender the advantage of a “physiologic” regulation according to the hormonal status of the recipient. Our method could therefore open up a new avenue for future experimentation that could influence the treatment of currently incurable diseases, including the osteopetrosis due to RANKL deficiency.

Acknowledgments

We are indebted to Dr. Rita Di Massimo for the excellent editing of this manuscript. This work was supported by the Telethon grant #GGP09018 and the Association Française contre les Myopathies grant AFM 2012 project #15889 SR.TH GENIQUE/CELL to AT, and by a Post-doctoral fellowship grant from the European Calcified Tissue Society to AC. AC, RP and AM were recipients of Marie Curie fellowships from the European Union funded project INTERBONE – FP7-PEOPLE-2011-IRSES -295181 to AT. AC, AM, RP and MC performed the experiments and collected the data. NR, MM and AT supervised the work. AC and AT wrote the paper. All Authors reviewed and approved the manuscript. Authors declare no conflict of interest.

References

[1] Sobacchi C, Schulz A, Coxon FP, Villa A, Helfrich MH. Osteopetrosis: genetics, treatment and new insights into osteoclast function. Nat Rev Endocrinol 2013;9:522–36.
[2] Sutton MT, Bonfield TL. Stem cells: innovations in clinical applications. Stem Cells Int 2014;2014:516278.
[3] Galderisi U, Giordano A. The gap between the physiological and therapeutic roles of mesenchymal stem cells. Med Res Rev 2014;34:1100–26.
[4] Mastri M, Lin H, Lee T. Enhancing the efficacy of mesenchymal stem cell therapy. World J Stem Cells 2014;6:82–93.
[5] Ito S, Hata T. Crystal structure of RANK ligand involved in bone metabolism. Vitam Horm 2004;67:19–33.
[6] Martin TJ. Historically significant events in the discovery of RANK/RANKL/OPG. World J Orthop 2013;4:186–97.
[7] Sims NA, Vrahnas C. Regulation of cortical and trabecular bone mass by communication between osteoblasts, osteocytes and osteoclasts. Arch Biochem Biophys 2014. pii: S0003-9861(14) 00172-6.
[8] Souza PP, Lerner UH. The role of cytokines in inflammatory bone loss. Immunol Invest 2013;42:555–622.
[9] Biskobing DM, Fan X, Rubin J. Characterization of MCSF-induced proliferation and subsequent osteoclast formation in murine marrow culture. J Bone Miner Res 1995;10:1025–32.
[10] Arai F, Miyamoto T, Ohneda O, Inada T, Sudo T, Brasel K, et al. Commitment and differentiation of osteoclast precursor cells by the sequential expression of c-Fms and receptor activator of nuclear factor kappaB (RANK) receptors. J Exp Med 1999;190:1741–54.
[11] Hanada R, Hanada T, Sigl V, Schramek D, Penninger JM. RANKL/RANK-beyond bones. J Mol Med Berl 2011;89:647–56.
[12] Wong BR, Josien R, Lee SY, Sauter B, Li HL, Steinman RM, et al. TRANCE (tumor necrosis factor [TNF]-related activation-induced cytokine), a new TNF family member predominantly expressed in T cells, is a dendritic cell-specific survival factor. J Exp Med 1997;186:2075–80.
[13] Danks L, Takayanagi H. Immunology and bone. J Biochem 2013;154:29–39.
[14] Fata JE, Kong YY, Li J, Sasaki T, Irie-Sasaki J, Moorehead RA, et al. The osteoclast differentiation factor osteoprotegerin-ligand is essential for mammary gland development. Cell 2000;103:41–50.
[15] Schramek D, Leibbrandt A, Sigl V, Kenner L, Pospisilik JA, Lee HJ, et al. Osteoclast differentiation factor RANKL controls development of progestin-driven mammary cancer. Nature 2010;468:98–102.
[16] Hanada R, Leibbrandt A, Hanada T, Kitaoka S, Furuyashiki T, Fujihara H, et al. Central control of fever and female body temperature by RANKL/RANK. Nature 2009;462:505–9.
[17] Hikita A, Tanaka S. Ectodomain shedding of receptor activator of NF-kappaB ligand. Adv Exp Med Biol 2007;602:15–21.
[18] Sobacchi C, Frattini A, Guerrini MM, Abinun M, Pangrazio A, Susani L, et al. Osteoclast-poor human osteopetrosis due to mutations in the gene encoding RANKL. Nat Genet 2007;39:960–2.
[19] Villa A, Guerrini MM, Cassani B, Pangrazio A, Sobacchi C. Infantile malignant, autosomal recessive osteopetrosis: the rich and the poor. Calcif Tissue Int 2009;84:1–12.
[20] Guerrini MM, Sobacchi C, Cassani B, Abinun M, Kilic SS, Pangrazio A, et al. Human osteoclast-poor osteopetrosis with hypogammaglobulinemia due to TNFRSF11A (RANK) mutations. Am J Hum Genet 2008;83:64–76.
[21] Hsu H, Lacey DL, Dunstan CR, Solovyev I, Colombero A, Timms E, et al. Tumor necrosis factor receptor family member RANK mediates osteoclast differentiation and activation induced by osteoprotegerin ligand. Proc Natl Acad Sci U S A 1999;96:3540–5.
[22] Takayanagi H. Osteoimmunology and the effects of the immune system on bone. Nat Rev Rheumatol 2009;5:667–76.
[23] Cappariello A, Maurizi A, Veeriah V, Teti A. The great beauty of the osteoclast. Arch Biochem Biophys 2014;558C:70–8.
[24] Osteopetrosis. Consensus guidelines for diagnosis, therapy and follow-up. http://masonshafferfoundation.org/wp-content/uploads/2012/06/Osteopetrosis-Guidelines-2011.pdf.
[25] Kong YY, Feige U, Sarosi I, Bolon B, Tafuri A, Morony S, et al. Activated T cells regulate bone loss and joint destruction in adjuvant arthritis through osteoprotegerin ligand. Nature 1999;402:304–9.
[26] Kim N, Odgren PR, Kim DK, Marks Jr SC, Choi Y. Diverse roles of the tumor necrosis factor family member TRANCE in skeletal physiology revealed by TRANCE deficiency and partial rescue by a lymphocyte-expressed TRANCE transgene. Proc Natl Acad Sci U S A 2000;97:10905–10.
[27] Lo Iacono N, Blair HC, Poliani PL, Marrella V, Ficara F, Cassani B, et al. Osteopetrosis rescue upon RANKL administration to Rankl(-/-) mice: a new therapy for human RANKL-dependent ARO. J Bone Miner Res 2012;27:2501–10.
[28] Minkin C. Bone acid phosphatase: tartrate-resistant acid phosphatase as a marker of osteoclast function. Calcif Tissue Int 1982;34:285–90.
[29] Bab I, Ashton BA, Syftestad GT, Owen ME. Assessment of an in vivo diffusion chamber method as a quantitative assay for osteogenesis. Calcif Tissue Int 1984;36:77–82.
[30] Benayahu D, Gurevitch O, Zipori D, Wientroub S. Bone formation by marrow osteogenic cells (MBA-15) is not accompanied by osteoclastogenesis and generation of hematopoietic supportive microenvironment. J Bone Miner Res 1994;9:1107–14.
[31] Yang XB, Bhatnagar RS, Li S, Oreffo RO. Biomimetic collagen scaffolds for human bone cell growth and differentiation. Tissue Eng 2004;10:1148–59.
[32] Edamura K, Itakura S, Nasu K, Iwami Y, Ogawa H, Sasaki N, et al. Xenotransplantation of porcine pancreatic endocrine cells to total pancreatectomized dogs. J Vet Med Sci 2003;65:549–56.
[33] Nakashima T, Hayashi M, Fukunaga T, Kurata K, Oh-Hora M, Feng, et al. Evidence for osteocyte regulation of bone homeostasis through RANKL expression. Nat Med 2011;17:1231–4.
[34] Hikita A, Yana I, Wakeyama H, Nakamura M, Kadono Y, Oshima Y, et al. Negative regulation of osteoclastogenesis by ectodomain shedding of receptor activator of NF-kappaB ligand. J Biol Chem 2006;281:36846–55.
[35] Murphy G, Knauper V. Relating matrix metalloproteinase structure to function: why the “hemopexin” domain? Matrix Biol 1997;15:511–8.
[36] Lynch CC, Hikosaka A, Acuff HB, Martin MD, Kawai N, Singh RK, et al. MMP-7 promotes prostate cancer-induced osteolysis via the solubilization of RANKL. Cancer Cell 2005;7:485–96.

[37] Lum L, Wong BR, Josien R, Becherer JD, Erdjument-Bromage H, Schlöndorff J, et al. Evidence for a role of a tumor necrosis factor-alpha (TNF-alpha)-converting enzyme-like protease in shedding of TRANCE, a TNF family member involved in osteoclastogenesis and dendritic cell survival. J Biol Chem 1999;274:13613–8.
[38] Saengdee P, Chaisriratanakul W, Bunjongpru W, Sripumkhai W, Srisuwan A, Jeamsaksiri W, et al. Surface modification of silicon dioxide, silicon nitride and titanium oxynitride for lactate dehydrogenase immobilization. Biosens Bioelectron 2014. pii: S0956-5663(14)00558-2.
[39] Sabbota AL, Kim HR, Zhe X, Fridman R, Bonfil RD, Cher ML. Shedding of RANKL by tumor-associated MT1-MMP activates Src-dependent prostate cancer cell migration. Cancer Res 2010;70:5558–66.
[40] Yasuda H, Shima N, Nakagawa N, Yamaguchi K, Kinosaki M, Mochizuki S, et al. Osteoclast differentiation factor is a ligand for osteoprotegerin/osteoclastogenesis-inhibitory factor and is identical to TRANCE/RANKL. Proc Natl Acad Sci U S A 1998;95:3597–602.
[41] Del Fattore A, Peruzzi B, Rucci N, Recchia I, Cappariello A, Longo M, et al. Clinical, genetic, and cellular analysis of 49 osteopetrotic patients: implications for diagnosis and treatment. J Med Genet 2006;43:315–25.
[42] Supanchart C, Wartosch L, Schlack C, Kühnisch J, Felsenberg D, Fuhrmann JC, et al. ClC-7 expression levels critically regulate bone turnover, but not gastric acid secretion. Bone 2014;58:92–102.